JPE 18-3-18

https://doi.org/10.6113/JPE.2018.18.3.841
ISSN(Print): 1598-2092 / ISSN(Online): 2093-4718

Dual-Algorithm Maximum Power Point Tracking Control Method for Photovoltaic Systems based on Grey Wolf Optimization and Golden-Section Optimization

Ji-Ying Shi*, Deng-Yu Zhang*, Le-Tao Ling**, Fei Xue†, Ya-Jing Li*, Zi-Jian Qin***, and Ting Yang*

*Key Laboratory of Smart Grid of Ministry of Education, Tianjin University, Tianjin, China
**Shenzhen Power Supply Bureau, China Southern Power Grid, Shenzhen, China
†Electric Power Research Institute, State Grid Ningxia Electric Power Company, Yinchuan, China
***Laiwu Power Supply Bureau, State Grid Shandong Electric Company, Laiwu, China

Abstract

This paper presents a dual-algorithm search method (GWO-GSO) combining grey wolf optimization (GWO) and golden-section optimization (GSO) to realize maximum power point tracking (MPPT) for photovoltaic (PV) systems. First, a modified grey wolf optimization (MGWO) is activated for the global search. In conventional GWO, wolf leaders possess the same impact on decision-making. In this paper, the decision weights of wolf leaders are automatically adjusted with hunting progression, which is conducive to accelerating hunting. At the later stage, the algorithm is switched to GSO for the local search, which play a critical role in avoiding unnecessary search and reducing the tracking time. Additionally, a novel restart judgment based on the quasi-slope of the power-voltage curve is introduced to enhance the reliability of MPPT systems. Simulation and experiment results demonstrate that the proposed algorithm can track the global maximum power point (MPP) swiftly and reliably with higher accuracy under various conditions.

Key words: Golden-section optimization, Maximum power point tracking, Modified grey wolf optimization, Partial shading conditions, Photovoltaic systems

I. INTRODUCTION

To mitigate the international energy crisis and reduce environmental pollution, the exploitation of renewable energy is experiencing rapid growth around the world. Among various kinds of renewable energy, solar energy is considered to be an important energy source due to it being abundant, inexhaustible and environment-friendly. PV power generation has become an indispensable method for the utilization of solar energy. To harvest PV energy more efficiently, maximum power point tracking (MPPT) techniques are being developed. However, it is essential to tackle two major challenges in the application of a MPPT technique. On the one hand, the power-voltage characteristic curve of a PV array is nonlinear, which depends on solar irradiance and temperature [1]. On the other hand, under partial shading conditions (PSCs) due to clouds, buildings, trees, and so on, local maximum power points (MPP) can appear on the power-voltage curve because it is necessary to make the bypass diode in parallel with PV modules to avoid the hot spot effect [2].

On the whole, MPPT techniques consist of conventional and intelligent MPPT methods [3]. Conventional MPPT methods (including perturb and observe (P&O) [4], incremental conductance (INC) [5], GSO [6], beta method [7], etc.) have simple structures and low equipment requirement. However, these conventional methods can be immersed in local MPPs

Manuscript received Sep. 28, 2017; accepted Jan. 16, 2018
Recommended for publication by Associate Editor Jonghoon Kim.
†Corresponding Author: tjuxf1010@126.com
Tel: +86-022-2740-6071, State Grid Ningxia Electric Power Company
*Key Lab. of Smart Grid of Ministry of Education, Tianjin Univ., China
**Shenzhen Power Supply Bureau, China Southern Power Grid, China
***Laiwu Power Supply Bureau, State Grid Shandong Electric Co., China

© 2018 KIPE

under PSCs, which decreases the efficiency of a PV system. To improve conventional methods ability to track the actual global MPP under PSCs, several attempts have been suggested in the literature. For example, the authors of [8] reported a MPPT controller that uses a field programmable gate array (FPGA)-based real time INC. This method is capable of having excellent timing performance since one of the most important features of FPGA is the implementing of circuits by hardware description, which gives FPGA the highest timing performance when compared with DSPs, microcontrollers and even analogue circuits. The authors of [9] proposed a modified β-parameter-based method with an optimized scaling factor. However, due to the use of a PV emulator in its experiment, the sampling time for the MPPT controller is long since the PV emulator has dynamic constraints and a slower response speed than a practical crystalline PV.

Intelligent methods include PSO [10], [11], firefly algorithm (FA) [12], [13], cuckoo search (CS) [14], [15] and grey wolf optimization (GWO) [16]. These methods are capable of tracking the global MPP. However, intelligent methods are generally more complex and slower than conventional methods. Recently, a lot work has been done to optimize these algorithms [17]. The authors of [18] proposed a modified FA algorithm that uses the average position of all of the brighter fireflies as the representative point. As a result, the fireflies move toward this point without wandering toward all of the brighter flies. Furthermore, a boost converter with an interleaved topology is used as the dc–dc converter in this method to reduce ripple currents, improve reliability and increase efficiency. The authors of [19] described an optimal control scheme for the single-phase grid-connected PV systems under different fast variation shading patterns. The scheme combines the extended memory searching capabilities and adaptive inertia weight of the modified PSO. In this method, a PWM with permutations of the DC converter switching is applied to balance the switch utilization.

GWO is an intelligent algorithm proposed in 2014 by Mirjalili [20]. A large body of research has demonstrated that GWO shows satisfactory performance in various fields such as wind turbines [21], solar thermal power systems [22], large scale power systems [23] and smart grids [24]. Four merits of GWO can be summarized as: simplicity, flexibility, efficient exploitation and exploration [20]. This paper presents a dual-algorithm search method combining GWO and GSO to track the global MPP under various conditions. In the original GWO [16], wolf leaders possess the same impact on decision-making. In the proposed algorithm, the decision weights of the wolf leaders are automatically adjusted with hunting progression, which is helpful for hunting prey rapidly and efficiently. The concept of search density is also introduced as reference for deciding the maximum iteration and number of wolves. At the later stage, the algorithm is switched to the local search implemented by GSO, which is advantageous for avoiding unnecessary search and reducing the tracking time. In addition, conventional restart judgment based on the power change ratio can be invalid in the case of particular rapid changes in irradiation conditions. Therefore, a novel restart judgment based on the quasi-slope of power-voltage curve is introduced to enhance the reliability of MPPT systems.

Conventional MPPT control schemes usually consist of control loops and proportional integral (PI) controllers. However, such control schemes have the following defects [25]: complex structure; (2) time-consuming; and (3) the need to tune the PI gain. Furthermore, due to the nonlinear characteristics of PV systems and unpredictable environmental conditions, PI controllers are not appropriate for standalone PV systems [26]. In addition, MPPT controllers can be operated in the absence of control loops, which is known as the direct MPPT control scheme. The PI control loops are eliminated and the duty cycle is computed directly with algorithms. In this study, the direct MPPT control scheme based on the power–duty curve is adopted.

The rest of this paper is organized as follows. Section II briefly introduces the basics of GWO and GSO. Section III describes the proposed algorithm. Section IV and V present simulation and experiment results. Some conclusions are made in Section VI.

II. BASIC OF GWO AND GSO

A. GWO

GWO originates from the social hierarchy and hunting mechanism of grey wolves in nature. Grey wolves are inclined to live in a pack and the size of the pack is usually between 5 and 12. The size of the wolf pack in this paper is six. They have a rather strict social dominant hierarchy. Four types of grey wolves, alpha (α), beta (β), delta (δ), and omega (ω), are used to simulate the social hierarchy of a grey wolf whose dominance decreases from front to rear. Four main steps are implemented for realizing optimization in GWO, which are chasing, approaching, encircling and attacking. Encircling behavior can be modeled by the following equations:

$$\vec{D} = \left|\vec{C} \cdot \overrightarrow{X_{\mathrm{p}}}(t) - \vec{X}(t)\right| \tag{1}$$

$$\vec{X}(t+1) = \overrightarrow{X_{\mathrm{p}}}(t) - \vec{A} \cdot \vec{D} \tag{2}$$

where t is the current iteration, $\overrightarrow{X_{\mathrm{p}}}$ is the position vector of the prey, and $\vec{X}$ is the position vector of the grey wolf. $\vec{A}$ and $\vec{C}$ are the only intermediate coefficient vectors, which are obtained by:

$$\vec{A} = 2\vec{a} \cdot \overrightarrow{r_1} - \vec{a} \tag{3}$$

$$\vec{C} = 2 \cdot \overrightarrow{r_2} \tag{4}$$

Because $\vec{a}$ is decreased linearly from 2 to 0, the iteration

can be used as the intermediate variable. Consequently, $\vec{a}$ is described as:

$$\vec{a} = (-1/3) \times t + 7/3 \quad (5)$$

$\vec{a}$ decreases linearly from 2 to 0 during the course of optimization, and r_1 and r_2 are random vectors in [0, 1]. Consequently, $|\vec{A}|$ and $|\vec{C}|$ lie inside the interval of $[-|\vec{a}|, |\vec{a}|]$ and [0, 2], respectively. Wolves attack towards prey when $|\vec{A}| < 1$. When the values of $|\vec{A}|$ and $|\vec{C}|$ are bigger than 1, GWO shows random behavior to avoid being trapped in local optima. Grey wolves diverge from prey in hopes of finding better prey when $|\vec{A}| > 1$.

The hunting mechanism in GWO is dominated by the social hierarchy in a wolf pack. Specifically speaking, the three best wolves lead the wolf pack to hunt prey. In other words, the three best wolves are the leaders of the pack. In the next hunting, the positions of the wolf leaders are saved and the other wolves have to update their positions according to the positions of the wolf leaders. The positions of common wolves in the next iteration are proposed as follows:

$$\vec{D}_\alpha = |\vec{C}_1 \cdot \vec{X}_\alpha - \vec{X}| \quad (6)$$

$$\vec{D}_\beta = |\vec{C}_2 \cdot \vec{X}_\beta - \vec{X}| \quad (7)$$

$$\vec{D}_\delta = |\vec{C}_3 \cdot \vec{X}_\delta - \vec{X}| \quad (8)$$

$$\vec{X}_1 = |\vec{X}_\alpha - \vec{A}_1 \cdot (\vec{D}_\alpha)| \quad (9)$$

$$\vec{X}_2 = |\vec{X}_\beta - \vec{A}_2 \cdot (\vec{D}_\beta)| \quad (10)$$

$$\vec{X}_3 = |\vec{X}_\delta - \vec{A}_3 \cdot (\vec{D}_\delta)| \quad (11)$$

$$\vec{X}(t+1) = (\vec{X}_1 + \vec{X}_2 + \vec{X}_3)/3 \quad (12)$$

In this paper, search density is first introduced as reference for deciding the maximum iteration and number of wolves. The search density is defined as:

$$\rho = 1/(N_w \times t_{max}) \quad (13)$$

where ρ is the search density, N_w and t_{max} represent the number of wolves and the maximum number of iterations, respectively. A larger search density increases tracking efficiency but reduces the tracking speed. On the other hand, a small search density reduces the tracking time, but degrades search accuracy. A reasonable search density gives an optimal tradeoff between tracking time and tracking accuracy. After repeated simulations, the search density threshold is identified to be 0.03. In other words, the search density ρ must satisfy equation (14). In this paper, N_w is set to be six and t_{max} is set as 7. Therefore, the value of ρ is 0.0238.

$$\rho < \rho_0 \quad (14)$$

where ρ_0 is the search density threshold.

B. GSO

GSO is a classical solution to the single peak optimizing problem. A search interval [a, b] of length L is divided by two points X_1 and X_2, which must satisfy equation (15).

$$ax_2 = x_1 b = \lambda L \quad (15)$$

where the value of λ is equal to 0.618. After comparing the corresponding function values $f(X_1)$ and $f(X_2)$, GSO selects the next search space according to the following rules. If $f(X_1) < f(X_2)$, the maximum must lie in the range of [X_1, b], which is taken as a new interval for the next iteration. On the other hand, if $f(X_1) > f(X_2)$, [a, X_2] is taken in the next iteration. The new interval is always 0.618 times the original interval. The process is repeated continuously until the distance between X_1 and X_2 is less than a certain chosen precision.

III. Principle of Proposed Algorithm

The authors of [16] reported a MPPT scheme that uses GWO to track the global MPP. However, the method requires numerous iterations resulting in substantial power losses. Compared with the original GWO, three promising features of the proposed algorithm can be summarized as follows.

A. Automatically Adjusting the Decision Weights

In this paper, the size of the wolf pack is six and the best two wolves are selected to be the leaders of the pack. The two leaders of the pack are represented by α and β, which are considered to have better knowledge concerning the potential location of prey. In this paper, the global MPP is regarded as prey. In the beginning of the search, α and β possess the same influence in terms of leading the wolf pack. As the search advances, the decision weights of α and β are adjusted automatically to accelerate the tracking speed. Specifically, the decision weight of α becomes increasingly heavy and the decision weight of β becomes increasingly light as given by equations (19) and (20). This is helpful for speeding up the tracking. On the one hand, if the leaders possess the same decision weights all the time, there may be a delay in decision-making. On the other hand, after the decision weights are dynamically adjusted, the wolf pack possesses a more specific tracking target. In every iteration, the positions of α and β are saved and the rest of wolves are obliged to move their positions as follows:

$$\vec{D}_\alpha = |\vec{C}_1 \cdot \vec{X}_\alpha - \vec{X}|, \vec{D}_\beta = |\vec{C}_2 \cdot \vec{X}_\beta - \vec{X}| \quad (16)$$

$$\vec{X}_1 = |\vec{X}_\alpha - \vec{A}_1 \cdot (\vec{D}_\alpha)| \quad (17)$$

$$\vec{X}_2 = |\vec{X}_\beta - \vec{A}_2 \cdot (\vec{D}_\beta)| \quad (18)$$

$$W_1 = 1/2 + 1/2 \times (2^t - 2)/2^{t_{max}} \quad (19)$$

$$W_2 = 1/2 - 1/2 \times (2^t - 2)/2^{t_{max}} \quad (20)$$

$$\vec{X}(t+1) = W_1 \vec{X}_1 + W_2 \vec{X}_2 \quad (21)$$

In the search process, wolves jump to the place where prey is likely to exist. All of the wolves track the prey based on the encircling behavior of GWO. With the tracking advancing, the size of the encirclement comprising of the wolf pack

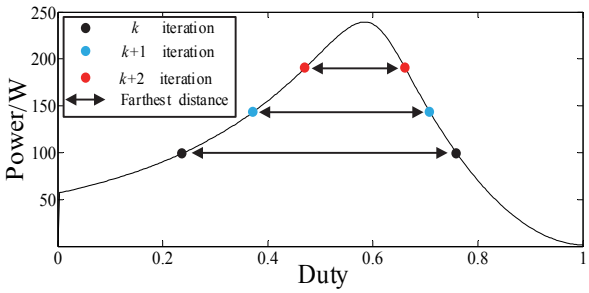

Fig. 1. Distance between the two farthest wolves as the exploitation narrows by degrees.

shrinks by degrees. The size of the encirclement is indicated by the distance between the two farthest wolves in the exploitation, which narrows by degrees as depicted in Fig. 1.

B. Local Search Stage

The algorithm is transformed from the global search to the local search when either of two conditions is achieved: the first one is reaching the maximum iteration; the second one is satisfying the judgment of successful hunting. The judgment of successful hunting is expressed by equation (22).

$$d_{1-2} \le 1/5N \tag{22}$$

where $d_{1\text{-}2}$ is the distance between α and β, and N is the number of PV modules in a series. It is considered that the desired prey is found when both α and β acquire the approximate position of the global MPP. Then tracking is switched to the local search. Otherwise, at the later stage, some of the wolves still attempt to explore for better prey, which is unnecessary and wastes a massive amount of tracking time. The local search is implemented by GSO. Before the algorithm enters GSO, the positions of two wolf leaders are selected to serve as initial search interval endpoints. However, it is possible that the global MPP does not lie within the initial search interval. Therefore, the initial search interval is expanded by d_{esi} as shown in Fig. 2. The formula for d_{esi} is written as:

$$d_{\text{esi}} = 2/5N \tag{23}$$

d_{esi} is large enough to ensure that the global MPP is covered in the initial search interval.

Due to the characteristic of GSO, the tracking time is shortened a lot and oscillation hardly exists in the steady state.

C. Modified Restart Judgment

If a PV system is severely affected by extrinsic factors, it is necessary to execute the procedure again to track a new global MPP. Detecting the power change ratio is one of the conventional restart judgments. It can be described as the scenario in which:

$$|(P_1 - P_0)/P_0| > \tau_0 \tag{24}$$

where P_0 is the power in the steady state, P_1 is the power in the next sampling period, and τ_0 is the restart tolerance.

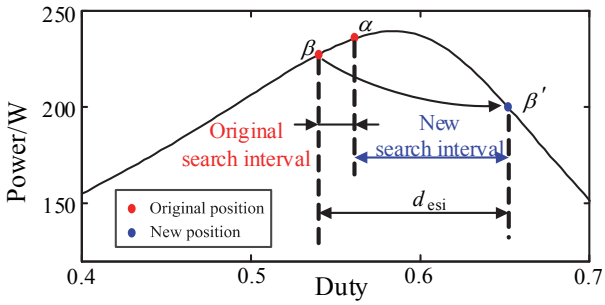

Fig. 2. Expanding the initial search interval of GSO.

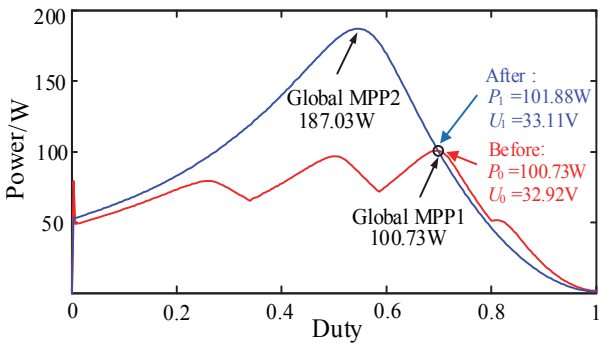

Fig. 3. Power-duty curve under a particular rapidly changing irradiation condition.

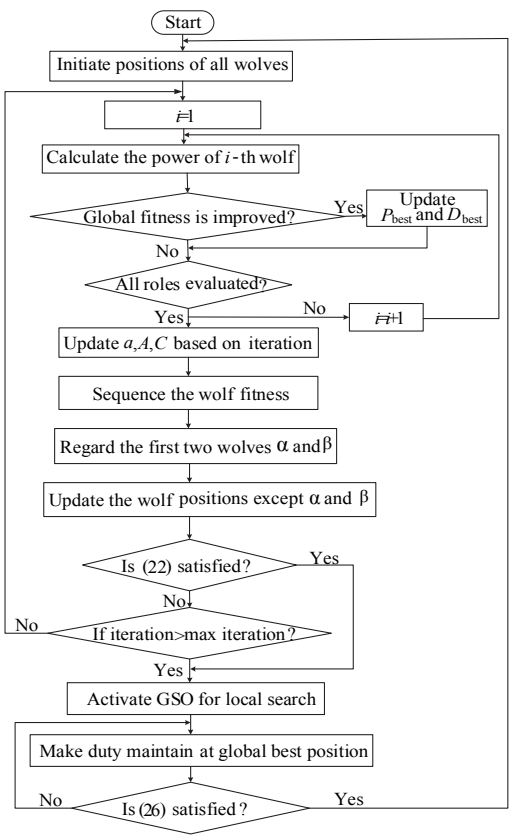

Fig. 4. Flowchart for the GWO-GSO algorithm.

However, it is possible for this restart judgment to be invalid when a tiny variation cannot be detected as given by:

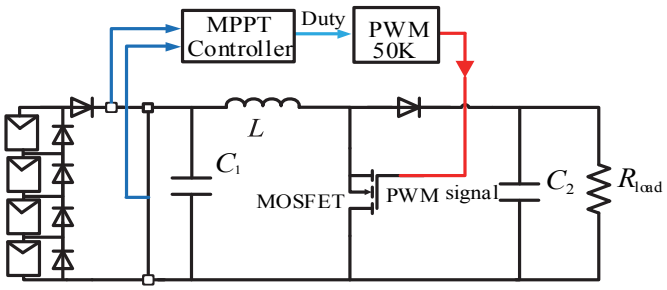

Fig. 5. Simulation model for a PV MPPT system.

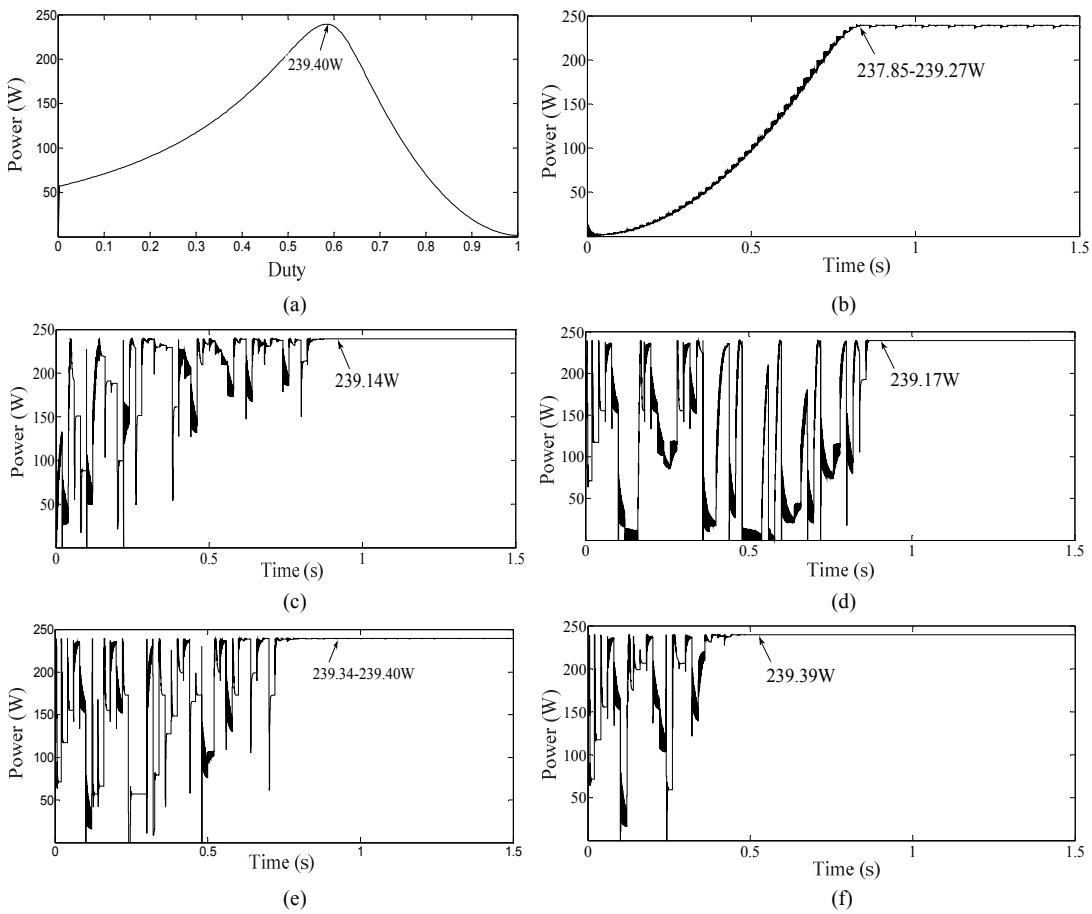

Fig. 6. (a) Power-duty curve, and tracking traces of: (b) P&O; (c) PSO; (d) GWO; (e) GWO-P&O; (f) GWO-GSO under uniform illumination condition.

$$\tau < \tau_0 \tag{25}$$

where τ is the power change ratio. Power-duty curve under a particular rapidly changing irradiation condition is depicted in Fig. 3. The value of τ is 0.001 in the case of Fig. 3, which is difficult to detect. Considering that the slope of the power-voltage curve can serve as a reference for restarting the algorithm, the quasi-slope of the power-voltage curve is introduced to enhance the reliability of the restart judgment, which is inspired by the INC. The quasi-slope can be described as:

$$|(P_1 - P_0)/(U_1 - U_0 + \mu)| > \varepsilon_0 \tag{26}$$

where the value of μ is set to be 0.001 to prevent a zero-denominator. The quasi-slope is 6.02 under the circumstance of Fig. 3, which is big enough to detect and restart. This allows the PV system to reliably detect variations in the irradiation condition and reduce power loss. The above-proposed improvement is summarized in the flowchart shown in Fig. 4.

IV. Simulation Results and Analysis

In order to verify the performance of the proposed algorithm, MATLAB/Simulink software is used to implement simulations. An equivalent model [27] replaces the PV module to carry out the simulation. The principal simulation

TABLE I
PRINCIPAL PARAMETERS OF THE FIVE ALGORITHMS

Algorithms	Adjustable parameters	Initial positions
P&O	$\Delta D = 0.01$	1.0
PSO	$N_p = 6, \omega = 0.5, c_1 = 0.5, c_2 = 1, t_{max} = 7$	0.1,0.3,0.4,0.6,0.7,0.9
GWO	$N_w = 6, t_{max} = 7, \tau_0 = 0.05$	0.1,0.3,0.4,0.6,0.7,0.9
GWO-P&O	$N_w = 6, t_{max} = 7, \Delta D_{GWO\text{-}P\&O} = 0.0015$	0.1,0.3,0.4,0.6,0.7,0.9
GWO-GSO	$N_w = 6, t_{max} = 7, \varepsilon_0 = 2$	0.1,0.3,0.4,0.6,0.7,0.9

TABLE II
COMPREHENSIVE PERFORMANCES OF THE FIVE ALGORITHMS UNDER UNIFORM ILLUMINATION CONDITIONS

Global MPP	Algorithms	Tracking power	Tracking time	Capable of tracking global MPP
239.40W	P&O	237.85-239.27W	0.82s	√
	PSO	239.14W	0.86s	√
	GWO	239.17W	0.86s	√
	GWO-P&O	239.34-239.40W	0.88s	√
	GWO-GSO	239.39W	0.52s	√

parameters of the model under STC are P_{max} = 60 W, V_{mp} = 17.1 V, I_{mp} = 3.5 A, U_{oc} = 21.1 V and I_{sc} = 3.8 A.

The simulation model for a PV MPPT system consists of five parts, including a PV string, boost circuit, MPPT control module, PWM 50kHz module and load as shown in Fig. 5. The components for the designed MPPT system are chosen as MOSFET Frequency f = 50 kHz, C_1 = 100 μF, L = 0.5 mH, C_2 = 100 μF and R_{load} = 120 Ω.

The results obtained with the GWO-GSO are compared with those from the P&O, PSO, GWO and GWO-P&O under various environmental conditions. It is necessary to ensure a fair comparison among these algorithms. Therefore, the numbers of particles and wolves are set to be identical. The principal parameters of the five algorithms are summarized in Table I. In this table, N_p and N_w are the numbers of particles and wolves, respectively. t_{max} represents the maximum number of iterations.

A. Uniform Illumination Condition

The irradiance of each module is 1000 W/m^2, and a single MPP exists in the corresponding power-duty curve as shown in Fig. 6(a), whose value is about 239.40 W. Tracking traces for the five algorithms are also shown in Fig. 6.

The comprehensive performances of the five algorithms are shown in Table II. It can be seen that the five algorithms all can reach the MPP. However, the steady-state efficiency of GWO-P&O is reduced due to the fixed-step size P&O at the later stage as shown in Fig. 6(e). Compared to PSO, GWO and GWO-P&O, the tracking time of the GWO-GSO is shortened by 39.53%, 39.53% and 40.91%, respectively.

B. Partial Shading Condition

The irradiance values of four PV modules are set as 300, 500, 850 and 1000 W/m^2, which is the most complicated situation for a 4×1 string. The corresponding power-duty curve under PSC is shown in Fig. 7(a). Four peaks exist in the curve, and the third peak is the global MPP whose value is about 100.73 W. The MPPT traces for the five algorithms are also shown in Fig. 7.

The comprehensive performances of the five algorithms are listed in Table 3. P&O converges to a local MPP because it is unable to discriminate between a local MPP and the global MPP. PSO, GWO, GWO-P&O and GWO-GSO achieve the goals of reaching the global MPP. The steady-state oscillation of GWO-P&O still exists due to the fixed-step size P&O as shown in Fig. 7(e). Compared to PSO, GWO and GWO-P&O, the tracking time of the GWO-GSO is reduced by 25.58%, 25.58% and 27.27% in this scenario.

C. Rapidly Changing Irradiation Conditions

A novel restart judgment is examined and analyzed in this scenario. A step change is set from PSC to uniform irradiation condition. Initially, the PV string is under PSC. The irradiance values of four PV modules under PSC are set as 300, 500, 850 and 1000 W/m^2. At t = 1.5 s, the isolation suddenly changes to uniform irradiation condition. The irradiance of each module under uniform irradiation condition is 810 W/m^2. The corresponding power-duty curve and the trails for these five algorithms are plotted in Fig. 8.

The comprehensive performances of the five algorithms are summarized in Table 4. In this scenario, P&O gets trapped in local MPP3 before t = 1.5 s. Subsequently, P&O is capable of tracking the global MPP because the irradiation condition is uniform after t = 1.5 s. However, PSO and GWO fail to restart because the conventional restart judgment cannot detect tiny variations in power as depicted in Fig. 8(c) and 8(d). GWO-P&O is capable of restarting and tracking the global MPP with the help of the perturbing in P&O. The proposed algorithm overcomes the drawbacks of the conventional restart judgment and responds accurately under

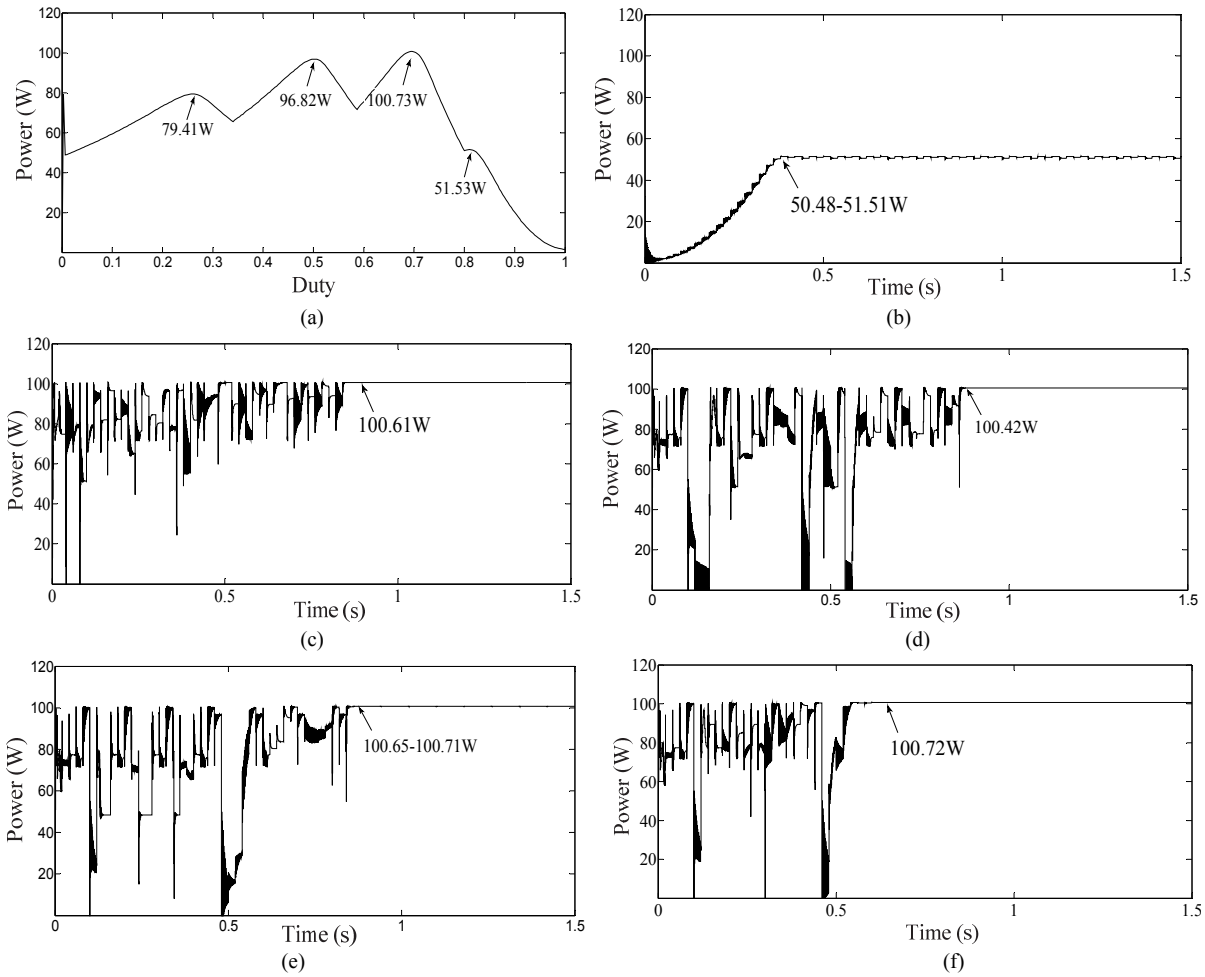

Fig. 7. (a) Power–duty curve, and tracking traces of: (b) P&O; (c) PSO; (d) GWO; (e) GWO-P&O; (f) GWO-GSO under PSC.

TABLE III
COMPREHENSIVE PERFORMANCES OF THE FIVE ALGORITHMS UNDER PSC

Global MPP	Algorithms	Tracking power	Tracking time	Capable of tracking global MPP
100.73W	P&O	50.48-51.51W	0.38s	×
	PSO	100.61W	0.86s	√
	GWO	100.42W	0.86s	√
	GWO-P&O	100.65-100.71W	0.88s	√
	GWO-GSO	100.72W	0.64s	√

TABLE IV
COMPREHENSIVE PERFORMANCES OF THE FIVE ALGORITHMS UNDER RAPIDLY CHANGING CONDITIONS

Global MPP		Algorithms	Tracking power		Tracking time		Capable of tracking global MPP	
Before	After		Before	After	Before	After	Before	After
100.73W	187.03W	P&O	50.48-51.51W	185.79-186.92W	0.38s	0.52s	×	√
		PSO	100.70W	103.25W	0.86s		√	×
		GWO	100.70W	103.35W	0.86s		√	×
		GWO-P&O	100.70-100.71W	187.00-187.01W	0.90s	1.00s	√	√
		GWO-GSO	100.57W	186.90W	0.54s	0.42s	√	√

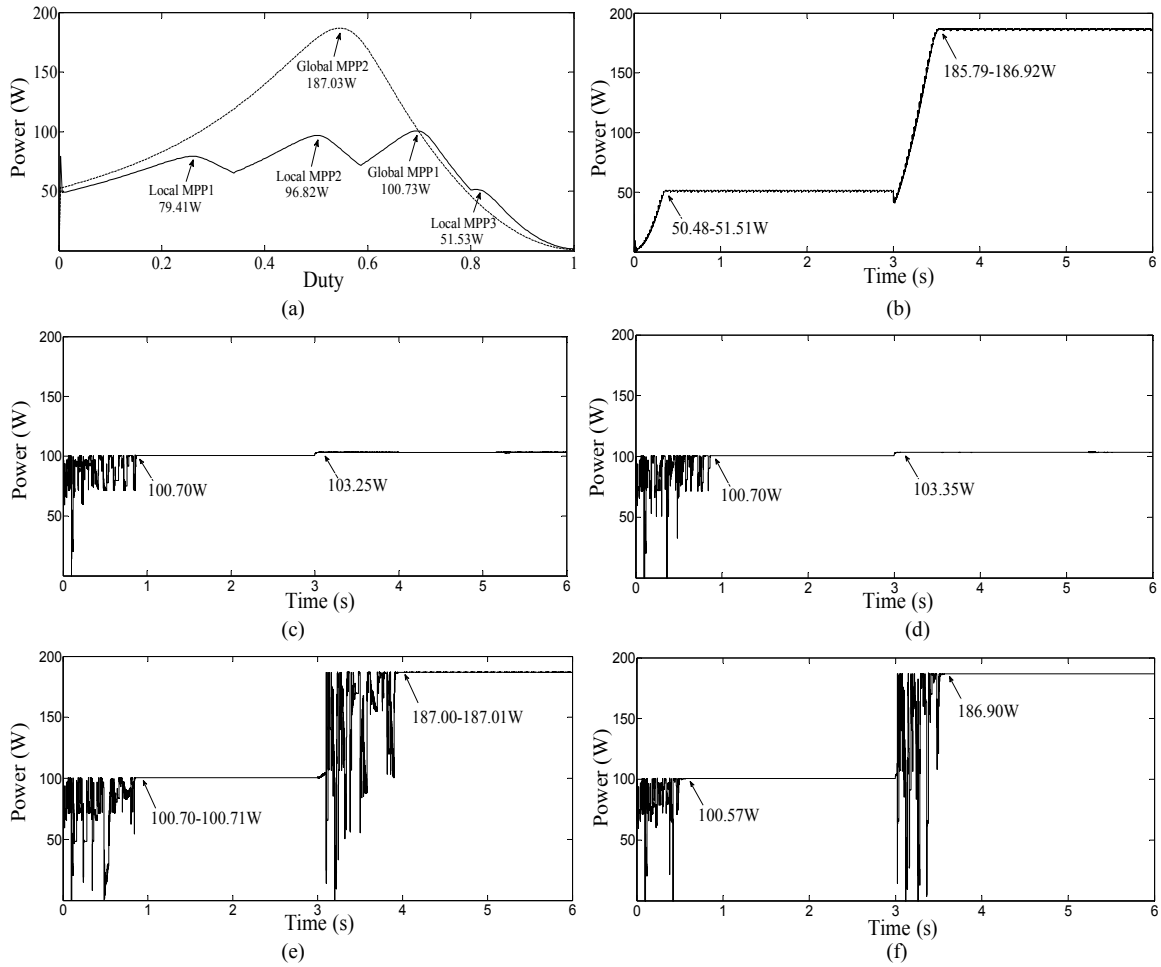

Fig. 8. The corresponding power-duty curve and the trails for these five algorithms. (a) Power–duty curve, and tracking traces of: (b) P&O; (c) PSO; (d) GWO; (e) GWO-P&O; (f) GWO-GSO under rapidly changing conditions.

irradiation changes as shown in Fig. 8(f). Furthermore, the GWO-GSO has the fastest tracking speed and the lowest power loss among all of the algorithms. Generally speaking, the GWO-GSO clearly outperforms the other four algorithms in this scenario.

V. Experimental Results

The experimental devices consist of a PV string (4×1), a DC-DC boost converter, a purely resistive load, and a DSP (Digital Signal Processor) (TI TMS320F28335), which is used to execute MPPT algorithms. Solar panels are used in the experiment with the following specifications: the maximum power of a solar panel (under STC) P_{MPP} = 100 W, voltage at MPP V_{MPP} = 18.48 V, current at MPP I_{MPP} = 5.41 A, open circuit voltage V_{OC} = 22.92 V and short circuit current I_{SC} = 5.70 A. The specifications of the main components for the boost converter are the same as those in the simulation. A picture of the experimental setup is shown in Fig. 9.

A current sensor (CC65) is used to sense the current of the PV string I_{pv}. The voltage of the PV string V_{pv} can be acquired directly from the voltage divider circuit of the PV string. The V_{pv} and I_{pv} signals are transmitted to the DSP via sensor circuits and A/D converters. Then optimization algorithms are implemented by the DSP, which sends out a PWM signal to the gate driver for controlling the MOSFET switch. The switching frequency of the boost converter is 50 kHz. Therefore, the MPPT sampling period for the experiment is 20 μs. The MPPT sampling period is set as an identical value to compare the performances of these algorithms fairly.

Fig. 9. Picture of the experimental setup.

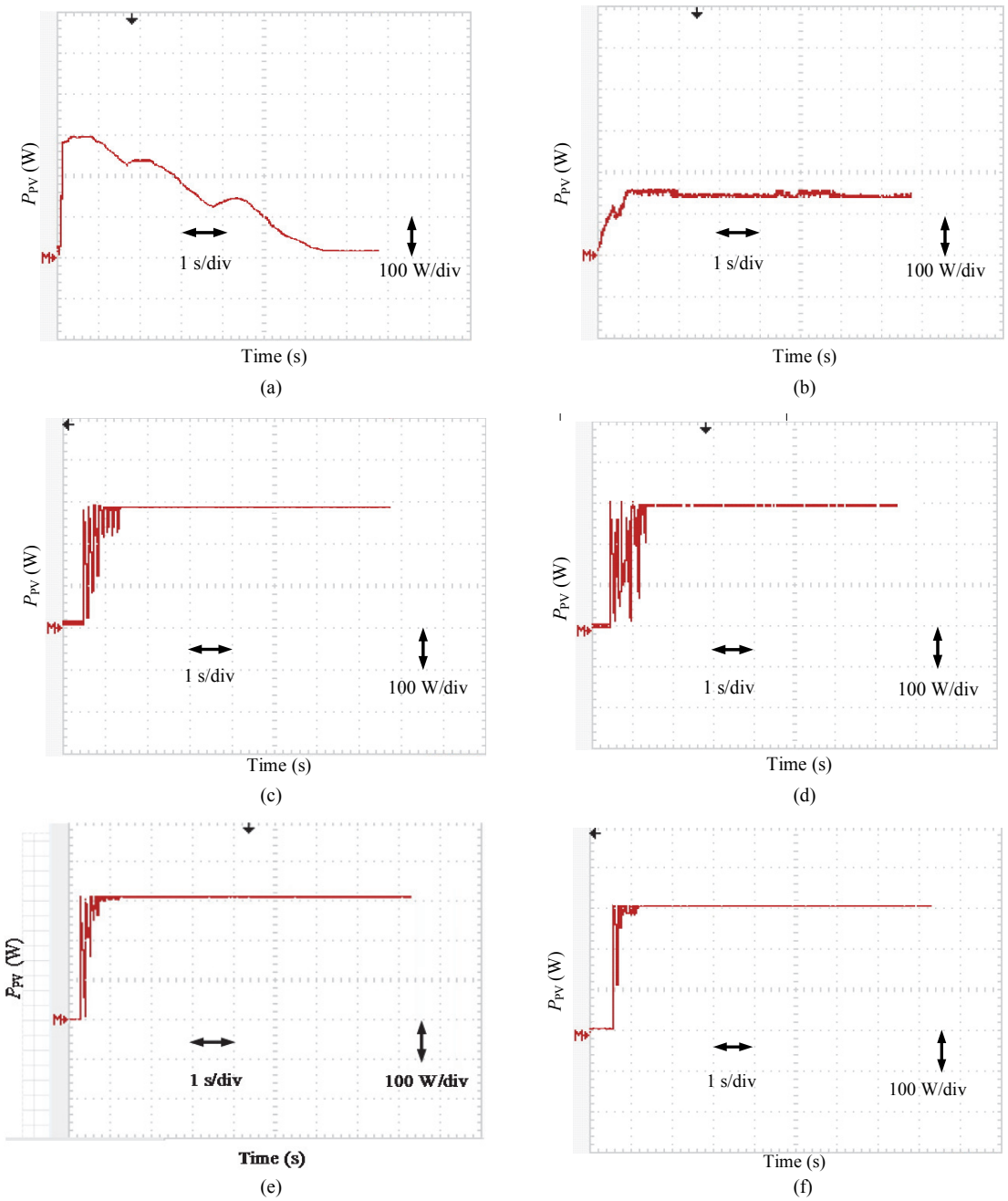

Fig. 10. Experimental waveforms: (a) Power–duty curve, and the tracking trajectories of: (b) P&O; (c) PSO; (d) GWO; (e) GWO-P&O; (f) GWO-GSO under PSC.

To validate the proposed algorithm, a case under PSC is investigated. In order to create PSC, PV modules are shaded with different semi-transplant films (12mm). Fig. 10(a) provides the power-duty curve under PSC, which is obtained by utilizing global scanning, where the scan step size is chosen as 0.01. In P&O, ΔD=0.01; in PSO, the number of particles is N_p =6, ω=0.5, c_1 =0.5, c_2 =1.0 and t_{max}=7; in GWO, the number of wolves is N_w =6, t_{max}=7, τ_0 =0.05; in GWO-P&O, the number of wolves is N_w =6, t_{max}=7, the step length is 0.0015; in the GWO-GSO, the number of wolves is N_w =6, t_{max}=7, ε_0 =2. The experimental tracking trajectories of the five algorithms are shown in Fig. 10.

It is easy to confirm that P&O gets trapped in a local MPP as shown in Fig. 10(a). PSO, GWO, GWO-P&O and the GWO-GSO successfully find the global MPP. It takes about 0.86s, 0.86s, 0.88s and 0.54s to track the global MPP by using PSO, GWO, GWO-P&O, and the GWO-GSO, respectively. After satisfying the judgment of successful hunting, the proposed algorithm is switched to the local search and thus saving a lot of tracking time. The judgment of successful hunting can reduce inefficient searching and unnecessary iterations, which shortens the tracking time by

37.21% in this case. Fig. 10 indicates that the tracking time of the GWO-GSO is the shortest among all of the algorithms. Therefore, the experiment results verify that the proposed algorithm has a higher tracking speed and tracking accuracy in comparison with P&O, PSO, GWO and GWO-P&O.

VI. CONCLUSIONS

This paper introduces a dual-algorithm search method for MPPT and demonstrates its ability to extract the global MPP. Simulation and experiment results show that the tracking time of the proposed algorithm is greatly reduced due to variations in the decision weights and the mechanism of successful hunting. The extracted power also becomes higher due to the local search implemented by GSO at the later stage. In addition, a novel restart judgment based on the quasi-slope of the power-voltage curve enhances the reliability of a MPPT system. In terms of tracking time and output power, the proposed GWO-GSO exhibits better performance than P&O, PSO, GWO and GWO-P&O under various conditions.

ACKNOWLEDGMENT

This paper is supported by the National Key Research and Development Program of China (2017YFB0903000); National Natural Science Foundation of China (61571324); Natural Science Foundation of Tianjin (16JCZDJC30900); and National Program of International S&T Cooperation (2013 DFA11040).

REFERENCES

[1] M. Zouli, S. Ghoudelbourk, A. Ouari, and D. Dib, "Influence of the external and internal parameters on the characteristics of generator PV," *AIP Conference Proceedings*, Vol. 1814, No. 1, pp. 020007, Feb. 2017.

[2] T. Logeswaran and A. SenthilKumar, "A review of maximum power point tracking algorithms for photovoltaic systems under uniform and non-uniform irradiances," *Energy Procedia*, Vol. 54, No. 2014, pp. 228-235, Jul. 2014.

[3] S. Saravanan and N. R. Babu, "Maximum power point tracking algorithms for photovoltaic system – A review," *Renewable and Sustainable Energy Reviews*, Vol. 57, No. 2016, pp. 192-204, May. 2016.

[4] L. Piegari, R. Rizzo, I. Spina, and P. Tricoli, "Optimized adaptive perturb and observe maximum power point tracking control for photovoltaic generation," *Energies*, Vol. 8, No. 5, pp. 3418-3436, Apr. 2015.

[5] R. Faraji, A. Rouholamini, H. R. Naji, R. Fadaeinedjad, and M. R. Chavoshian, "FPGA-based real time incremental conductance maximum power point tracking controller for photovoltaic systems," *IET Power Electronics*, Vol. 7, No. 5, pp. 1294-1304, Oct. 2013.

[6] A. Kheldoun, R. Bradai, R. Boukenoui, and A. Mellit, "A new Golden Section method-based maximum power point tracking algorithm for photovoltaic systems," *Energy Conversion and Management*, Vol. 111, No. 2016, pp. 125-136, Jan. 2016.

[7] X. Li, H. Wen, L. Jiang, Y. Hu, and C. Zhao, "An Improved Beta Method With Autoscaling Factor for Photovoltaic System," *IEEE Trans. Ind. Appl.*, Vol. 52, No. 5, pp. 4281-4291, Sep. 2016.

[8] Y. Tian, B. Xia, Z. Xu, and W. Sun, "Modified asymmetrical variable step size incremental conductance maximum power point tracking method for photovoltaic systems," *J. Power Electron.*, Vol. 14, No. 1, pp. 156-164, Jan. 2014.

[9] X. Li, H. Wen, L. Jiang, E. G. Lim, Y. Du, and C. Zhao, "Photovoltaic modified β-parameter-based MPPT method with fast tracking," *J. Power Electron*, Vol. 16, No. 1, pp. 9-17, Jan. 2016.

[10] M. Seyedmahmoudian, S. Mekhilef, R. Rahmani, R. Yusof, and A. A. Shojaei, "Maximum power point tracking of partial shaded photovoltaic array using an evolutionary algorithm: A particle swarm optimization technique," *J. Renew. Sustain. Energy*, Vol. 6, No. 2, pp. 023102, Mar. 2014.

[11] K. H. Chao, "A high performance PSO-based global MPP tracker for a PV power generation system," *Energies*, Vol. 8, No. 7, pp. 6841-6858, Jul. 2015.

[12] K. Sundareswaran, S. Peddapati, and S. Palani, "MPPT of PV systems under partial shaded conditions through a colony of flashing fireflies," *IEEE Trans. Energy Convers*, Vol. 29, No. 2, pp. 463-472, Jun. 2014.

[13] J. Y. Shi, F. Xue, Z. J. Qin, L. T. Ling, T. Yang, Y. Wang and J. Wu, "Tracking the global maximum power point of a photovoltaic system under partial shading conditions using a modified firefly algorithm," *J. Renew. Sustain. Energy*, Vol. 8, No. 3, pp. 033501, May 2016.

[14] J. Ahmed, Z. Salam, "A maximum power point tracking (MPPT) for PV system using cuckoo search with partial shading capability," *Applied Energy*, Vol. 119, No. 2014, pp. 118-130, Jan. 2014.

[15] J. Y. Shi, F. Xue, Z. J. Qin, W. Zhang, L. T. Ling, and T. Yang, "Improved global maximum power point tracking for photovoltaic system via cuckoo search under partial shaded conditions," *J. Power Electro.n*, Vol. 16, No. 1, pp. 287-296, Jan. 2016.

[16] S. Mohanty, B. Subudhi, and P. K. Ray, "A new MPPT design using grey wolf optimization technique for photovoltaic system under partial shading conditions," *IEEE Trans. Sustain. Energy*, Vol. 7, No. 1, pp. 181-188, Jan. 2016.

[17] D. Verma, S. Nema, A. M. Shandilya, and S. K. Dash, "Maximum power point tracking (MPPT) techniques: Recapitulation in solar photovoltaic systems," *Renew. Sustain. Energy Rev.*, Vol. 54, No. 2016, pp. 1018-1034, Nov. 2015.

[18] M. Mao, L. Zhang, Q. Duan, and B. Chong, "Multilevel

DC-link converter photovoltaic system with modified PSO based on maximum power point tracking," *Solar Energy*, Vol. 153, No. 2017, pp. 329-342, Jun. 2017.

[19] D. Teshome, C. H. Lee, Y. W. Lin, and K. L. Lian, "A modified firefly algorithm for photovoltaic maximum power point tracking control under partial shading," *IEEE J. Emerg. Sel. Topics Power Electron.*, Vol. 5., No. 2, pp. 661-671, Jun. 2017

[20] S. Mirjalili, S. M. Mirjalili, and A. Lewis, "Grey wolf optimizer," *Advances in Engineering Software*, Vol. 69, No. 2014, pp. 46-61, Dec. 2014.

[21] B. Yang, X. S. Zhang, T. Yu, H. C. Shu, and Z. Fang, "Grouped grey wolf optimizer for maximum power point tracking of doubly-fed induction generator based wind turbine," *Energy Conversion and Management*, Vol. 133, No. 2017, pp. 427-443, Nov. 2016.

[22] Y. Sharma and L. C. Saikia, "Automatic generation control of a multi-area ST–Thermal power system using Grey Wolf Optimizer algorithm based classical controllers," *Int. J. Electrical Power Energy Syst.*, Vol. 73, No. 2015, pp. 853-862, Jun. 2015.

[23] D. Guha, P. K. Roy, and S. Banerjee, "Load frequency control of large scale power system using quasioppositional grey wolf optimization algorithm," *Eng. Sci. Technol.*, Vol. 19, No. 2016, pp. 1693-1713, Jul. 2016.

[24] W. Han, X. Shen, E. Hou, and J. Xu, "Precision time synchronization control method for smart grid based on wolf colony algorithm," *Int. J. Electr. Power Energy Syst.*, Vol. 78, No. 2016, pp. 816-822, Jan. 2016.

[25] K. Ishaque, Z. Salam, A. Shamsudin, and M. Amjad, "A direct control based maximum power point tracking method for photovoltaic system under partial shading conditions using particle swarm optimization algorithm," *Applied Energy*, Vol. 99, No. 2012, pp. 414-422, Jun. 2012.

[26] F. Salem, M. S. A. Moteleb, and H. T. Dorrah, "An enhanced fuzzy-PI controller applied to the MPPT problem," *J. Sci. Eng*, Vol. 8, No. 2, pp. 147-153, Jan. 2005.

[27] V. J. Chin, Z. Salam, and K. Ishaque, "An accurate modelling of the two-diode model of PV module using a hybrid solution based on differential evolution," *Energy Convers. Manag.*, Vol. 124, No. 2016, pp. 42-50, Jul. 2016.

Ji-Ying Shi was born in Tianjin, China, in 1959. He received his M.S. and Ph.D. degrees from Tianjin University, Tianjin, China, in 1993 and 1996, respectively. He was a Visiting Scholar and a Postdoctoral Researcher at the Hong Kong University of Science and Technology, Hong Kong, China, from July 1996 to November 1999. He is presently working as an Associate Professor of Electrical Engineering and Automation at Tianjin University. His current research interests include power electronic techniques, renewable energy, and soft switching techniques.

Deng-Yu Zhang was born in Hengshui, China, in 1993. He received his B.S. degree in Aeronautical Automation from the Civil Aviation University of China, Tianjin, China, in 2016. He is presently working toward his M.S. degree at Tianjin University, Tianjin, China. His current research interests include maximum power point tracking technology, renewable energy and power electronic techniques.

Le-Tao Ling received his M.S. degree from Tianjin University, Tianjin, China, in 2018. He is presently working for the Shenzhen Power Supply Bureau, China Southern Power Grid (CSG), Shenzhen, China. His current research interests include the maximum power point tracking of photovoltaic and wind power systems, renewable energy and power electronic techniques.

Fei Xue was born in Guyuan, China, in 1994. He received his B.S. and M.S. degrees in Electrical Engineering from Tianjin University, Tianjin, China, in 2014 and 2017, respectively. He is presently working as an Engineer in Electric Power Research Institute, State Grid Ningxia Electric Power Company (NEPC), Ningxia, China. His current research interests include maximum power point tracking technology, renewable energy, and the modeling and planning of distribution networks.

Ya-Jing Li received her B.S. degree in Electrical Engineering and Automation from Yanshan University, Qinhuangdao, China. She is presently working towards her M.S. degree at Tianjin University, Tianjin, China. Her current research interests include the modeling and planning of active distribution networks, renewable energy and power electronic techniques.

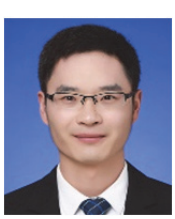

Zi-Jian Qin was born in Laiwu, China, in 1990. He received his M.S. degree from Tianjin University, Tianjin, China, in 2017. He is presently working for the Laiwu Power Supply Bureau, State Grid Shandong Electric Power Company, Laiwu, China. His current research interests include the modeling and simulation of microgrids and the maximum power point tracking of photovoltaic and wind energy generation systems.

Ting Yang is a Professor of Electrical Engineering at Tianjin University, Tianjin, China. He was a winner of the Education Ministry's New Century Excellent Talents Supporting Plan. Professor Yang is the author or co-author of four books, and more than 60 publications in technical journals and conference proceedings. He served as the chairman of two IEEE International Conference workshops. He is a Member of International Society for Industry and Applied Mathematics (SIAM), a Senior Member of the Chinese Institute of Electronic, and a Committee Member of Electronic Circuit and Systems. Professor Yang's current research interests include power electronic techniques and renewable energy.